Validation of the Kinetic Soot Model: An Experimental and Theoretical Study on Soot Formation using LII and SV-CARS

K.P. Geigle*, Y. Schneider-Kühnle, V. Krüger, M. Tsurikov, R. Lückerath, M. Braun-Unkhoff, N. Slavinskaya, P. Frank, W. Stricker, M. Aigner
DLR - Institut für Verbrennungstechnik, Stuttgart, Germany

Keywords: laser-induced incandescence, CARS, soot formation, kinetics

ABSTRACT: Temperature and soot concentration measurements from laminar, premixed flames at different conditions (pressures P, equivalence ratios ϕ and fuels), provide an excellent data base for the modelling of soot formation. For the verification of numerical simulations of sooting flames, the use of accurate, spatially and temporally resolved data measured with non-intrusive *in situ* measurement tools is necessary. We present the application of a recently developed technique for temperature measurements in sooting flames. Soot concentrations measured by laser-induced incandescence (LII) are compared to calculated profiles of soot formation, based on the measured temperatures. The overall agreement is quite satisfactory for the experimental conditions presented.

1 INTRODUCTION

Environmental concerns and decreasing pollutant emission limits are driving the need for a reduction of emissions such as soot. Therefore, fundamental understanding of soot formation and destruction is a current issue for industry and research. The first step to a better understanding is based on a separation of effects interacting in a complex way in realistic combustion systems. Thus, as one part of the problem, pure chemistry (no turbulence) needs to be investigated. Since chemistry is strongly dependent on temperature, the development and validation of a soot model needs accurate temperature information and soot concentrations measured under several flame conditions. Most practical combustion devices are operated at elevated pressure, but little data are available for flame experiments focusing on soot model validation at these conditions (Hanisch et al., 1994; Braun-Unkhoff et al., 1998). To provide the required information, we used laser-based, non-intrusive diagnostics which yield spatially-resolved data, necessary for resolving steep gradients. The main advantage of this approach over commonly-used line-of-sight techniques is that the assumption of a homogeneous distribution of the quantity of interest over large dimensions is not required (and in many flames not justified). The experiments are used to support kinetic computations in two respects. First, the measured temperature information is used for the calculation, thus including energy loss by radiation. Second, the predicted soot formation can be compared to the experimental soot volume fraction profiles. This comparison permits further refinement of the kinetic soot formation model.

2 EXPERIMENTAL SET-UP

2.1 *Burner configuration*

Validation experiments in high pressure flames for the support of a kinetic soot model without any influence of turbulence are a highly demanding challenge for burner design. First, a completely laminar flow resulting in a stable flame without flickering is required. In this case, a direct correlation of height above burner (HAB) with the time scale of the combustion process under study is possible. Furthermore, the flame needs to be sufficiently homogeneous over the measurement volume.

* *Corresponding author:* Klaus Peter Geigle, DLR – Institut für Verbrennungstechnik, Stuttgart, D-70569 Stuttgart, Germany. Email: klauspeter.geigle@dlr.de

For a comparison with 1D kinetical computations, any influence from the flame edges has to be excluded.

Our design, based on the requirements stated above, is similar to the ones described in Hanisch et al. (1994) and Jander et al. (1995). Its main feature is the use of a non-sooting shielding flame (d = 61.3 mm), surrounding the axisymmetric inner flame to be studied (d = 41.3 mm). The additional flame reduces oxidising influences from the flame edges and provides a hot shielding film against the surrounding cold coflowing air (d = 150 mm). Moreover, two separately operated flames are useful while changing flame conditions (P, ϕ, flow rates), since they behave as mutually pilot flames. Both flames were stabilised on water cooled sintered bronze matrices (cell size 12 µm). Additional flow conditioning and mixing of fuel and air was achieved by using glass beads below the matrices. For finding the required stable flames, the stoichiometries of both flames and the exit velocities of three cold gases (methane/air, fuel/air of studied flame, coflowing air) must be carefully adjusted. The flow rates, supplied by five in-house calibrated massflow controllers, are chosen to avoid horizontal flickering and vertical fluctuations, and to ensure a sufficiently homogeneous radial temperature and soot distribution within the detection volume of the used laser techniques. Premixing of the fuel and the corresponding air took place approximately one meter before the burner.

The entire burner inlet system was mounted into a high pressure housing with large windows for optical access. For further flame stabilisation, particularly at high pressures, a stabilising grid was positioned at a height of 40 or 45 mm above the burner plate, depending on the position of soot formation (Pape, 1993). For the experiments with toluene, the required combustion air was passed through a toluene bubbler consisting of several sealed bottles immersed in a water bath whose temperature was precisely controlled. A part of the air-toluene mixture was sampled and the toluene volume fraction determined *ex situ*. Each of the flame settings (Table 1) has been checked for reproducibility, the different measurements were usually performed the same day.

Table 1. Flame settings for the presented flames. All flow rates are in standard liters per minute. Pressure is in bars.

	Inner flame			Ring flame		Coflow	P		Inner flame			Ring flame		Coflow	P
Fuel	ϕ	Q_{fuel}	Q_{air}	Q_{CH4}	Q_{air}	Q_{air}		Fuel	ϕ	Q_{fuel}	Q_{air}	Q_{CH4}	Q_{air}	Q_{air}	
C_2H_4	2.30	0.7	4.4	1.0	4.6	110	1	C_3H_6	1.95	1.17	13	9.9	58	490	5
C_2H_4	2.30	1.7	11	5.7	38	390	3	C_3H_6	2.00	1.20	13	9.9	58	490	5
C_3H_6	2.23	0.3	3.1	1.5	11	200	1	C_3H_6	2.10	1.26	13	9.9	58	490	5
C_7H_8	1.88	0.064	1.5	1.9	11	98	1	C_3H_6	2.15	1.29	13	9.9	58	490	5

2.2 *Temperature measurements in sooting flames with SV-CARS*

While the use of thermocouples provides the easiest way of extracting temperature information from the flame, the accuracy in sooting flames is too low for model validation and, furthermore, any object introduced into the flame clearly disturbs the flame (Stricker, 2002). An ideal tool for *in situ*, non-intrusive temperature measurements in flames is Coherent Anti-Stokes Raman Scattering (CARS), which is based on measuring the population of rotational and vibrational energy levels of the nitrogen molecule (Eckbreth, 1996) and comparing these to simulated spectra. Conventional CARS uses the frequency-doubled output of a Nd:YAG laser (532 nm) for the pump beam. However, in a sooting flame, the exciting beams produce C_2 molecules from laser heated soot particles, which in turn cause fluorescence (Swan bands) at the same wavelength as the CARS signal (473 nm). Our approach is to use a narrowband dye laser (591 nm) for the pump beam, thus shifting the CARS signal out of the Swan band region. So the CARS signal is spectrally shifted from 473 nm to 520 nm resulting in completely undisturbed spectra (Fig. 1a). For non-sooting parts of a flame this shifted vibrational CARS signal was validated with conventional CARS, resulting in good agreement. The accuracy for SV-CARS measurements is ±3% (Schneider-Kühnle, 2003).

In our experiment, a frequency-doubled Nd:YAG laser was used to pump a narrowband dye laser and a custom-built broadband dye laser, whose beams were overlapped in BOXCARS geometry and focused to a 4 mm long, 0.2 mm wide probe volume. All beams were equipped with polarisers and half wave plates for intensity control; an additional analyser could be implemented for background suppression in the case of pressurised flames. Two translation stages allowed a fast shift of

the CARS measurement probe volume above the burner surface. The CARS signal was resolved in a spectrometer and detected with an intensified CCD camera.

2.3 *Soot distributions with laser-induced incandescence*

An excellent tool for *in situ* non-intrusive measurements of soot distributions is provided by laser-induced incandescence (LII), based on the emission of blackbody radiation resulting from strong laser induced heating of soot particles. In recent years, LII has matured into a reliable tool for the measurement of qualitative soot distributions and, with calibration, even for quantitative measurements in flames (Santoro and Shaddix, 2002). For calibration, an extinction measurement is typically performed. Uncertainties in the exact knowledge of the refractive index of soot, particularly at the position of the calibration measurement (Choi et al., 1994), determine the accuracy of calibration via extinction. To ensure a proper excitation especially in strongly sooting absorbing flames we used a power meter to monitor the energy in the laser sheet after it passed through the flame.

For excitation of the LII signal we used the 1064 nm output of a Nd:YAG laser. A set of sheet forming optics and a rectangular aperture produced a homogeneous excitation sheet of approximately 30 mm in height and 170 µm in width. The laser power was tuned by a half wave plate followed by a polariser to keep an energy of close to 35 mJ/pulse behind the flame. The LII signal was filtered at 450 nm and detected with an intensified CCD camera with two-frame capability. During the first gate immediately before the laser pulse, the flame luminosity was detected. The second gate of 40 ns duration over the laser pulse was used for detection of the signal.

For the extinction measurement the same optical pathway was used by the 532 nm output of the laser at low power (0.2 mJ/pulse in the sheet) to avoid processes other than extinction in the flame. Before entering the burner chamber a part of the laser sheet was reflected into a reference dye cell. The rest of the sheet was partially absorbed by the flame and afterwards refocused to a second dye cell. The use of an additional mirror in front of the CCD camera and changing to a 700 nm interference filter allows the detection of an extinction profile immediately after the LII measurement with the same camera. This approach is applicable since the measurement object is temporally stable. In contrast to other published data, where the integral extinction over the whole flame is measured (Axelsson et al., 2001) our set-up allows us to choose the best height for the calibration. While in the lowest regions of the flame extinction by soot is low, absorption by other species might influence the extinction measurement in a non-negligible way (Choi et al., 1994). Furthermore, in the region of initial soot production the soot properties are the least representative for the whole flame and not well known. High in the flame soot particles start aging, which again changes the optical properties. For data analysis we used the region between these extremes where the determined calibration constant remains stable (as indicated in Figure 1b).

Since in strongly sooting flames the effect of signal trapping is not negligible, we followed the approach described in Bryce et al. (2000) to correct for signal losses by absorption in the flame. The refractive index used in the data analysis was 1.60 – 0.59i (Charalampopoulos and Felske, 1987). A change of optical pathways necessary for the mentioned techniques (CARS, LII, extinction) took only a few seconds by using the aforementioned translation stage system (Fig. 2a).

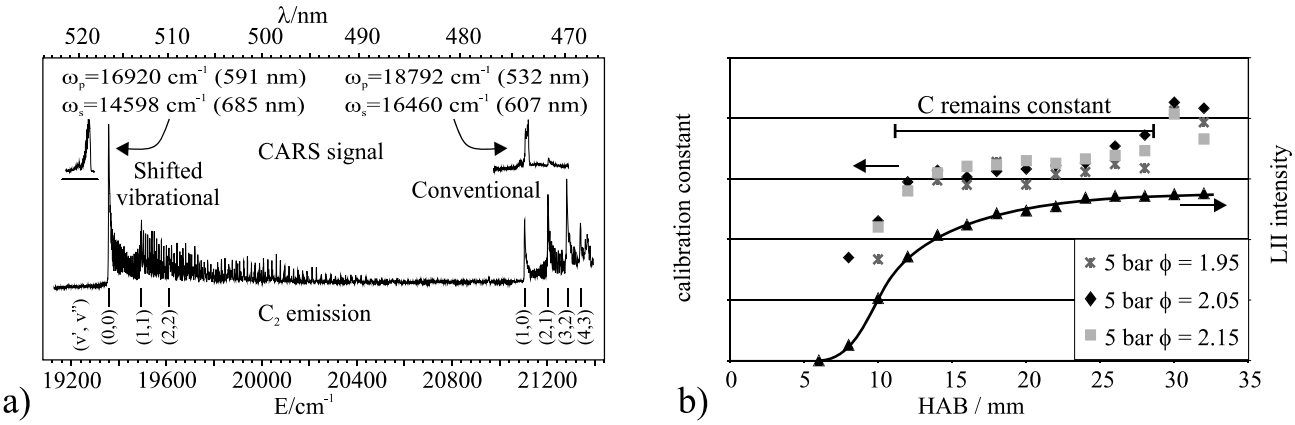

Figure 1. a) Spectral position of the conventional and the SV-CARS signal in the C_2 Swan-Band system. b) Variation of the calibration constant with height in different propene/air flames at 5 bar. Also shown for comparison is a LII signal intensity profile for the ϕ = 2.15 flame.

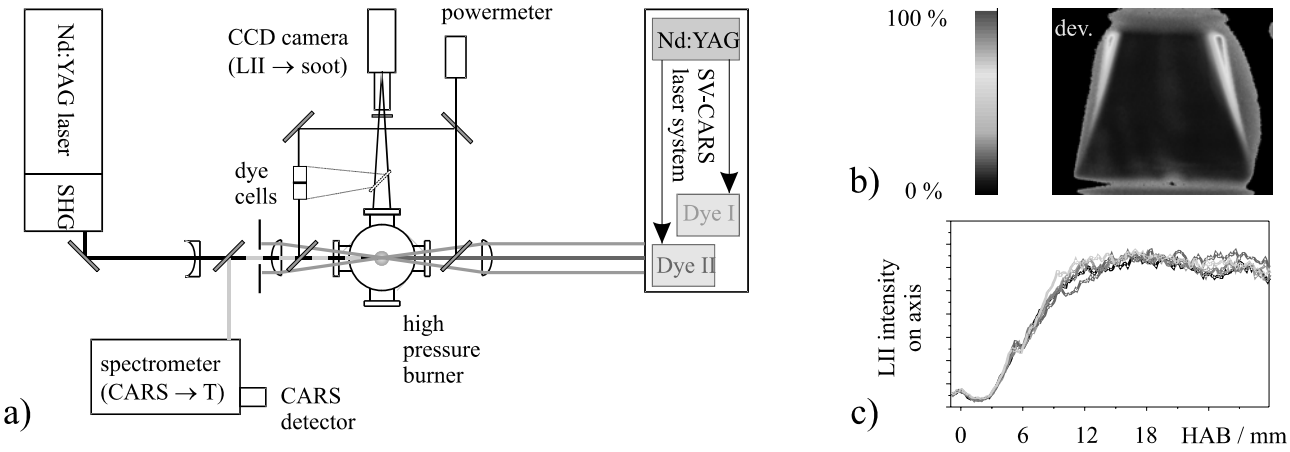

Figure 2a. Experimental set-up; translation stages enable a quick change between SV-CARS, LII and extinction measurements. b and c: Stability of the studied flames demonstrated for a 3 bar ethene/air flame; the upper image shows the standard deviation over a sequence of 100 LII images, the lower image displays some subsequently detected LII profiles along the burner axis.

3 KINETIC SOOT MODEL

At present, detailed modelling of soot formation and destruction is executed by using a relatively large gas phase reaction mechanism - including an improved model which contains detailed chemistry for PAH growth - coupled with a mechanistic soot model for particle inception, coagulation of particles, condensation, surface growth by gaseous species and soot particle oxidation (based on Frenklach and Wang, 1994).

A recently published reaction mechanism (Wang and Frenklach, 1997), which comprises the reactions of aromatic species up to pyrene, was updated by taking into account results obtained by shock tube experiments, especially on reactions of toluene, phenol, phenylacetylene, cyclopentadiene, propargyl and phenyl and benzyl radicals (Hu et al., 1999). This updated mechanism was validated by modelling the concentration profiles measured in a laminar, sooting ethene/O_2/Ar flame operated at atmospheric pressure (Harris et al., 1988). Measured species profiles of C_1-, C_2- and first aromatic ring compounds were reproduced very well.

As the base model for calculating the measured soot volume fraction f_v, the original soot model (Frenklach and Wang, 1994) was applied without any changes. This soot model describes PAH growth by linear lumping in which reactions of hydrocarbons with different numbers of condensed 6C rings (ranging from 3 to 7) are described by a replicating HACA (Hydrogen Abstraction Carbon Addition) reaction sequence. Particle inception occurs via PAH coagulation, starting with A4 (pyrene, $C_{16}H_{10}$). Further growth of the particles proceeds by coagulation of the particles and by surface growth controlled by reactions of the soot surface with OH and O_2.

One aim of the present study was to replace the PAH growth described by the HACA sequence by a comprehensive reaction mechanism which contains detailed kinetics for PAH species including the elementary reaction steps used in the HACA sequence. A reaction mechanism from MIT (Richter et al., 1999) comprising detailed kinetics to form species up to C_{30} was chosen. All the large PAHs formed in the PAH growth model were assumed to collide giving rise to nuclei: different combinations of PAH monomers are assumed to collide and form dimers; in a second step, these dimers collide with other monomers or dimers producing trimers etc. If the growing PAH has an amu > 760, a nucleus is born (Hu et al., 2000).

4 RESULTS AND DISCUSSION

Several flames using different fuels at different equivalence ratio and pressure were studied. LII intensity fluctuations in the central part of the flames typically remain below 15 % indicating sufficiently stable objects of measurement (Fig. 2b, c). Figure 3a shows the results for a 1 bar ethene/air

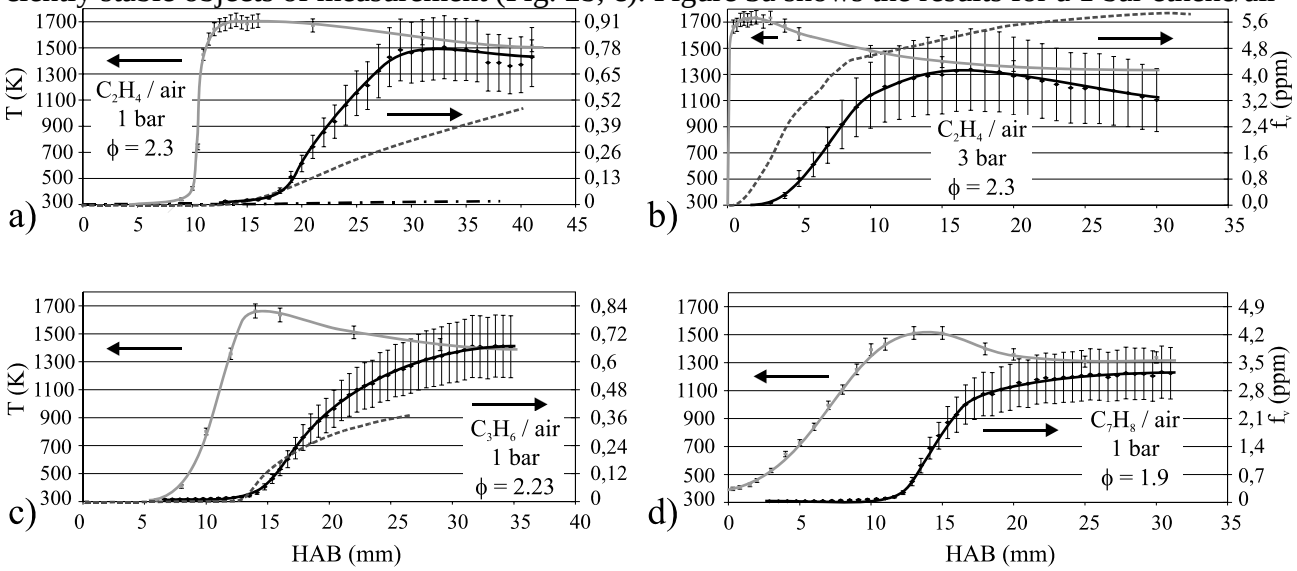

Figure 3. Measured temperature profiles (left scale) and soot volume fractions (right scale) for laminar premixed flames under the indicated conditions. Apart from the toluene flame (d) the actual kinetic computation results containing detailed gas phase chemistry are shown (dashed line). For the upper left flame (a) additionally a comparison with the pure HACA mechanism (dash dotted) is visible.

flame at ϕ=2.3. The figure shows measured soot volume fraction and temperature as a function of HAB, along with soot volume fraction results from the kinetic soot model. The soot plateau level of 0.8 ppm fits into the set of measurements of Jander et al. (1995) and Axelsson et al. (2001). The used soot model which was improved in the present work especially with respect to the growth of PAH, gives better agreement with measured soot concentration profiles than the initial soot model by Frenklach and Wang (1994) that used only the lumped HACA mechanism (alternating H-abstraction and C_2H_2 addition) for PAH growth. This is caused by an increased particle inception predicted by the detailed model for PAH growth as a consequence of the increased rate of soot precursor formation and thus that of particles. A comparison of our measured temperatures with published temperatures for similar flames is not useful. Temperatures depend strongly on flow speed (losses to the burner plate) and radiative losses to the specific surroundings. Additionally, the published results are based on thermocouple data or line of sight measurements thus not providing the accuracy and spatial resolution to be used as input for simulations. Our CARS measurements resulted in peak temperatures of 1715 K. Evidence for radiative energy loss is given by the downstream temperature decrease. When performing statistical analysis of 600 single CARS spectra, even in the very steep temperature rise, the single pulse temperature distribution at one location is shown to be relatively narrow (±100 K), proof of the excellent temporal and spatial stability of this flame and excluding height fluctuations of the reaction zone larger than 0.5 mm.

A clear benefit of the experimental set-up for simulations is to be emphasised: Even a lifted flame can be stabilised above the matrix surface by using the second (ring) flame. Thus, temperature measurements below the reaction zone can be performed resulting in well known starting conditions for the modelling.

It should be mentioned that the existence of a spatially resolved temperature profile measured with high accuracy is of great advantage with respect to the soot modelling especially as pressure increases and the reaction zone becomes very thin as in Figure 3a. Because temperature dominates the onset of soot formation, it is clear that modelling dynamic soot formation requires a realistic temperature profile between burner surface and post flame zone (Hu et al., 2000).

Increasing the pressure changes the profiles dramatically (Fig. 3b). At the lowest accessible height of 0.3 mm the temperature is already higher than 1600 K, indicating that the reaction takes place immediately above the burner surface. Absence of C_2 interferences at these high soot levels indicates the full functionality and reliability of the modified technique. At 3 bar the detected peak temperature was 1730 K, similar to the 1 bar case. At 2 mm above the reaction zone the soot concentration begins to rise, achieving a maximum of 4 ppm at 14 mm HAB.

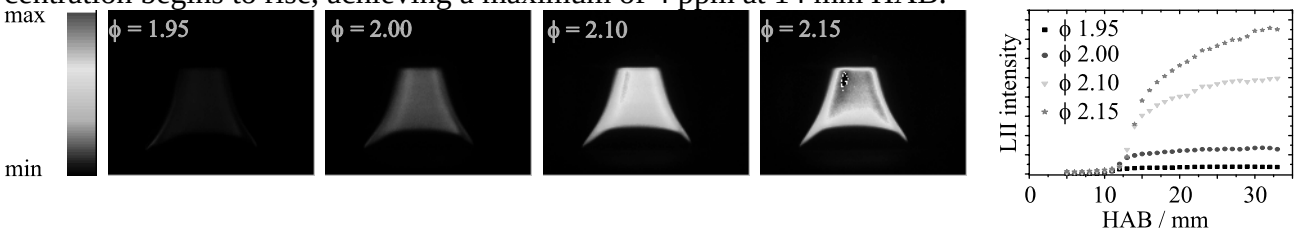

Figure 4. Soot distributions and vertical profiles upon change of the equivalence ratio for propene/air flames at 5 bar, not corrected for LII signal scattered at the burner surface.

These plateau soot volume fractions result in more than 30 % absorption of emitted LII signal, giving evidence to the need of correction for signal trapping.

For this flame, the starting conditions, i.e. the temperature at HAB = 0 for kinetic calculations, are not as well defined as in the 1 bar case. For the simulation a linear interpolation was performed between the first measured temperature and estimated room temperature at the burner surface. While the position of the soot rise is predicted too low, the slope of the calculated profile is in good agreement with the experiments and the final soot level is overestimating the measured values. Nevertheless, the overall agreement is satisfying.

Changing the fuel to propene does not dramatically influence the shape of the measured profiles (Fig. 3c). As for ethene, a lifted propene flame could be stabilised at atmospheric pressure and even the measured plateau soot level of 0.7 ppm is similar. The measured peak temperature is close to 1660 K. As in the former examples, there is good agreement of the calculated soot volume fraction with the measured one, clearly showing the correct trends.

Increasing the pressure to 5 bar resulted in significant problems in flame stabilisation. Even though the outer flame shape remained stable, the best achieved flames exhibited fluctuations of 1 – 2 mm at the lower edge and pronounced soot streaks at randomly changing positions. This caused unacceptable fluctuations in the CARS spectra, preventing accurate temperature measurements (i.e. narrow distribution at one position). Averaging 100 LII images removed the streaky structures completely, providing satisfactory qualitative information. Figure 4 shows LII images at 5 bar with inner flame ϕ=1.95 to 2.15. Since only the inner fuel flow rate was varied slightly (by less than 1 % of the total inner flow rate), the overall flow conditions are about the same for all flames. The richer the flame is the higher the plateau soot level.

The main components of aeroengine fuel are aliphatic hydrocarbons based on the above described ones. Even for longer chained hydrocarbons, the reaction mechanisms are not expected to be completely different. At lower concentrations available in the fuel but exhibiting higher soot forming potential, aromatic hydrocarbons are an essential object of interest for chemical kinetics. In particular, conventional models are based on soot formation over aromatic hydrocarbons after an initial fuel fragmentation. Thus, a direct study of an aromatic compound as fuel gives additional insight into the process of soot formation and the role of these species in the network of chemical reactions. As representative of aromatic molecules, toluene was chosen. Using the aforementioned liquid bubbler system, a laminar premixed toluene/air flame was stabilised at atmospheric conditions (Fig. 3d). Two main differences to the above described profiles are obvious: First, the temperature rise is much slower, proceeding over 8 mm and reaching a maximum of 1500 K, approximately 300 K below the adiabatic temperature for ϕ = 1.9, caused by the very low flow speed accompanied by radiative losses. Second, the plateau soot level is much higher indicating the large soot formation potential of aromatic compounds.

5 CONCLUSIONS

For the measurement of accurate model validation data the need for spatially resolved, *in situ*, non-intrusive measurement methods has been addressed. The presented work describes the application of a modified CARS excitation scheme for temperature determination in sooting flames (SV-CARS) in combination with soot volume fraction measurements by LII. To obtain a comprehensive data set for the soot model development and validation, accurate measurements of temperature and soot concentration have been performed in quasi 1D flames for ethene, propene, and toluene with various equivalence ratios and at pressures up to 5 bar. These experimental data could successfully be used for comparison with soot formation calculated by kinetic computations. The model predictions showed satisfactory agreement with the measurements; the main features of the measured soot profiles are correctly predicted. Further research is necessary with respect to the transition from PAH species to the first coagulating particles (e.g. incorporation of combinative reactions, Böhm et al., 2003) and to soot oxidation.

6 ACKNOWLEDGEMENTS

The authors want to thank Dr. R. Hadef for support during measurements and data analysis, funded by the Alexander von Humboldt-Foundation, the Helmholtz-Gemeinschaft Deutscher Forschungszentren (HGF) for funding during the research program “Particles and cirrus clouds” (PAZI), and M. Kapernaum for performing the volumetric analysis of the toluene mixture.

7 REFERENCES

Axelsson, B., R. Collin, P.E. Bengtsson, 2001: Laser-induced incandescence for soot particle size and volume fraction measurements using on-line extinction calibration. *Appl. Phys. B 72*, 367.

Böhm, H., M. Braun-Unkhoff, P. Frank, 2003: Investigations on initial soot formation at high pressures. *Progress in Computational Fluid Dynamics 3 (2-4)*, in press.

Braun-Unkhoff, M., A. Chrysostomou, P. Frank, E. Gutheil, R. Lückerath, W. Stricker, 1998: Experimental and numerical study on soot formation in laminar high-pressure flames. 27th Symp. (Int.) on Combustion, The Combustion Institute, Pittsburgh, p. 1565.

Bryce, D.J., N. Ladommatos, H. Zhao, 2000: Quantitative investigation of soot distribution by laser-induced incandescence. *Appl. Opt. 39*, 5012.

Choi, M.Y., A. Hamins, G.W. Mulholland, T.Kashiwagi, 1994: Simultaneous optical measurement of soot volume fraction and temperature in premixed flames. *Combustion and Flame 99*, 174.

Charalampopoulos, T.T., J.D. Felske, 1987: Refractive indices of soot particles deduced from in-situ laser light scattering measurements. *Comb. Flame 68*, 283.

Eckbreth, A.C., 1996: Laser diagnostics for combustion temperature and species. Overseas Publishers Association, Amsterdam B.V.

Frenklach, M., H. Wang, 1994: Detailed mechanism and modelling of soot particle formation. Springer-Verlag Berlin, Springer Series in Chemical Physics 59, 165.

Hanisch, S., H. Jander, T. Pape, H.G. Wagner, 1994: Soot mass growth and coagulation of soot particles in C_2H_4/air-flames at 15 bar. 25th Symp. (Int.) on Combustion, The Combustion Institute, Pittsburgh, p. 577.

Harris, S.J., A.M. Weiner, R.J. Blint, 1988: Formation of small aromatic molecules in a sooting ethylene flame. *Combust. Flame 72*, 91.

Hu, D., M. Braun-Unkhoff, P. Frank, 1999: Modelling study on soot formation at high pressures. *Combust. Sci. & Technol. 49*, 79.

Hu, D., M. Braun-Unkhoff, P. Frank, 2000: Modelling study on initial soot formation at high pressures. *Z. Phys. Chem. 214 (4)*, 473.

Jander, H., N. Petereit, D.M. Razus, 1995: The influence of carbon density on soot growth in atmospheric C_2H_4 (air, O_2)-flames. *Z. Phys. Chem. 188*, 159.

Pape, T., 1993: Optische Untersuchungen zum Rußwachstum in vorgemischten Ethen-Luft Flammen bei 15 bar. Diplom-Thesis, Göttingen, 17 pp.

Richter, H., W.J. Grieco, J.B. Howard, 1999: Formation mechanism of polycyclic aromatic hydrocarbons and fullerenes in premixed benzene flames. *Combust. Flame 119*, 1.

Santoro, R.J., C.R. Shaddix, 2002: Laser-induced incandescence. In: Applied Combustion Diagnostics [K. Kohse-Höinghaus, J.B. Jeffries (eds.)]. Taylor & Francis, New York, 252, and references therein.

Schneider-Kühnle, Y., 2003: Experimentelle Untersuchung rußender Hochdruckflammen mit Laserdiagnostischen Messmethoden. PhD Thesis, DLR Stuttgart, in progress.

Stricker, W., 2002: Measurement of temperature in laboratory flames and practical devices. In: Applied Combustion Diagnostics [K. Kohse-Höinghaus, J.B. Jeffries (eds.)]. Taylor & Francis, New York, 155.

Wang, H., M. Frenklach, 1997: A detailed kinetic modelling study of aromatics formation in laminar premixed acetylene and ethylene flames. *Combust. and Flame 110*, 173.